12th International Conference on Applications of Statistics and Probability in Civil Engineering, ICASP12
Vancouver, Canada, July 12-15, 2015

Geotechnical Reliability-based Designs and Links with LRFD

B. K. Low
School of CEE, Nanyang Technological University, Singapore

K. K. Phoon
Department of CEE, National University of Singapore, Singapore

ABSTRACT: Reliability-based design (RBD) can play a useful complementary role to overcome some limitations in the Load and Resistance Factor Design (LRFD) approach, for example in situations where loads contribute not only destabilizing but also stabilizing effects, situations where load and resistance sensitivities vary due to different geometric and other details, situations with modeling of spatial variability and parametric correlations, and situations with different targets of probability of failure. Examples of reliability-based design and analysis are presented to show that under the above circumstances RBD can offer interesting and enlightening insights apart from suggesting back-calculated load and resistance factors. When statistical information is available, direct FORM analysis can also be performed on the design resulting from LRFD, to obtain estimated probability of failure. Illustrative examples of FORM RBD and FORM analysis in this study consist of a shallow footing design, an anchored sheet pile wall design, a laterally loaded pile with depth dependent nonlinear p-y curves, and a clay slope with anisotropic and spatially autocorrelated undrained shear strength.

1. INTRODUCTION

The Hasofer-Lind (1974) index β is:

$$\beta = \min_{\mathbf{x}\in F} \sqrt{(\mathbf{x}-\boldsymbol{\mu})^T \mathbf{C}^{-1} (\mathbf{x}-\boldsymbol{\mu})} \tag{1a}$$

or, equivalently:

$$\beta = \min_{\mathbf{x}\in F} \sqrt{\left[\frac{x_i-\mu_i}{\sigma_i}\right]^T \mathbf{R}^{-1} \left[\frac{x_i-\mu_i}{\sigma_i}\right]} \tag{1b}$$

where $\mathbf{x}$ is a vector of random variables x_i, $\boldsymbol{\mu}$ the vector of mean values μ_i, $\mathbf{C}$ the covariance matrix, $\mathbf{R}$ the correlation matrix, σ_i the standard deviation, and F the failure domain.

An intuitive grasp of the Hasofer-Lind reliability index is provided by the multivariate normal distribution and its link to the Hasofer-Lind index:

$$f(\mathbf{x}) = \frac{1}{(2\pi)^{\frac{n}{2}} |\mathbf{C}|^{0.5}} \exp\left[-\frac{1}{2}(\mathbf{x}-\boldsymbol{\mu})^T \mathbf{C}^{-1} (\mathbf{x}-\boldsymbol{\mu})\right]$$
$$= \frac{1}{(2\pi)^{\frac{n}{2}} |\mathbf{C}|^{0.5}} \exp\left[-\frac{1}{2}\beta^2\right] \tag{2}$$

where β is defined by Eq. (1), without the "min". As a multivariate normal dispersion ellipsoid expands, its surfaces are contours of decreasing probability values. Hence, to minimize β (or β^2 in the above multivariate normal distribution) is to maximize the value of the multivariate normal probability density function, and to find the smallest ellipsoid tangent to the limit state surface (Fig. 1) is equivalent to finding the most probable failure point (the *design point*). This intuitive and visual understanding of the *design point* is consistent with the more mathematical approach in Shinozuka (1983, equations 4, 41, and Fig. 2), in which all variables were transformed into their standardized forms and the limit state equation had also to be written in terms of the standardized variables.

The first-order reliability method (FORM) can be regarded as an extension of the Hasofer-Lind index to cases involving correlated nonnormal distributions. In FORM, one can rewrite Eq. (1b) as follows (Low and Tang (2004)), and regard the computation of β as that

$$\text{LRFD Load factor} = \frac{\text{Design load}}{\text{Nominal load}}$$

Nominal load = Conservative load, > Mean value

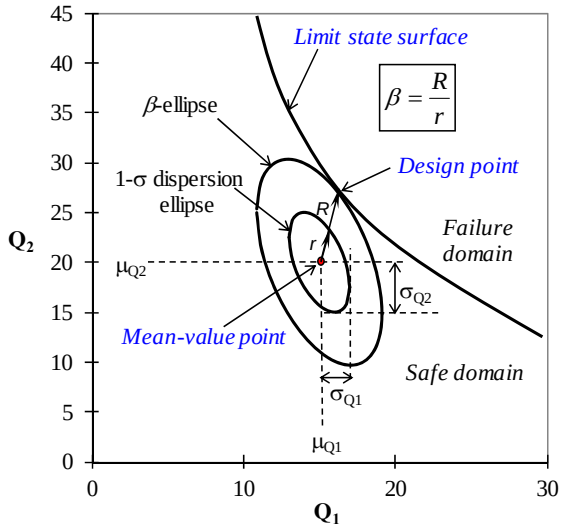

Figure 1: Dispersion ellipses and reliability index in the original space of normally distributed and correlated random variables. For correlated nonnormal random variables, the same perspective holds in terms of equivalent mean-value point and equivalent dispersion ellipsoids.

of finding the smallest *equivalent hyperellipsoid* (centered at the equivalent normal mean-value point $\boldsymbol{\mu}^N$ and with equivalent normal standard deviations $\boldsymbol{\sigma}^N$) that is tangent to the limit state surface (LSS):

$$\beta = \min_{\mathbf{x}\in F} \sqrt{\left[\frac{x_i - \mu_i^N}{\sigma_i^N}\right]^T \mathbf{R}^{-1} \left[\frac{x_i - \mu_i^N}{\sigma_i^N}\right]} \qquad (3)$$

where μ_i^N and σ_i^N can be calculated by the Rackwitz-Fiessler (1978) transformation. Hence, for correlated nonnormals, the ellipsoid perspective still applies in the original coordinate system, except that the nonnormal distributions are replaced by an equivalent normal ellipsoid, centered not at the original mean values of the nonnormal distributions, but at the equivalent normal mean $\boldsymbol{\mu}^N$.

Equation (3) was used in the Low and Tang (2004) FORM procedure. Another alternative was the Low and Tang (2007) Excel Solver

Low and Tang 2007 FORM procedure:
minimize β by varying **n,** on which **x** depends

$$\beta = \min_{\mathbf{x}\in F} \sqrt{\mathbf{n}^T \mathbf{R}^{-1} \mathbf{n}}$$

Use Excel's Solver to *minimize* β by changing the **n** vector, *subject to the constraint* g(**x**) = 0.

For each value of n_i tried by Solver, a short and simple Excel VBA code automates the computation of x_i from n_i, via

$$x_i = F^{-1}[\Phi(n_i)]$$

for use in the constraint g(**x**) = 0.

```
Function x_i(DistributionName, para, ni) As Double
 a1 = para(1):  a2 = para(2):  a3 = para(3):  a4 = para(4)
  Select Case UCase(Trim(DistributionName))
    Case "NORMAL":      x_i = a1 + ni * a2
    Case "LOGNORMAL"
       lamda = Log(a1) - 0.5 * Log(1 + (a2 / a1) ^ 2)
       zeta = Sqr(Log(1 + (a2 / a1) ^ 2))
       x_i = Exp(lamda + zeta * ni)
    Case "EXTVALUE1": …
    Case "EXPONENTIAL": …
    Case "UNIFORM":    …
    Case "TRIANGULAR": …
    Case "WEIBULL":    …
    Case "GAMMA": …
    Case "PERTDIST":   …
    Case "BETADIST":   …
End Select
End Function
```

Figure 2: Excel Solver procedure for FORM. The simple Excel codes for obtaining x_i from n_i for cases with distributions from Extreme Value (Gumbel) to Beta General are shown in Low and Tang (2007).

FORM procedure, Fig. 2, which recast Eq. (3) as follows:

$$\beta = \min_{\mathbf{x}\in F} \sqrt{\mathbf{n}^T \mathbf{R}^{-1} \mathbf{n}} \qquad (4)$$

The vector **n** is related to the **u** vector in the rotated and transformed space of the classical FORM procedure by:

$$\mathbf{n} = \mathbf{L}\mathbf{u} \;; \quad \mathbf{u} = \mathbf{L}^{-1}\mathbf{n} \qquad (5)$$

where **L** is the lower triangular matrix of the Cholesky decomposition of **R.** For each value of n_i tried by Excel Solver, a short and simple Excel

VBA code (Fig. 2) automates the computation of x_i from n_i for use in the constraint g(**x**) = 0, via $x_i = F^{-1}\left[\Phi(n_i)\right]$, where Φ is the standard normal cumulative distribution and *F* is the original nonnormal distribution, thereby obviating the need to compute μ_i^N and σ_i^N.

The FORM analyses in this paper are done using the Low and Tang (2007) **n**-space procedure. Other FORM software can also be used. The classical FORM procedure in **u**-space is explained in Ang and Tang (1984), Haldar and Mahadevan (1999) and Melchers (1999), among others. Recent studies of LRFD design are Foye et al. (2006), Bathurst et al. (2008), Fenton et al. (2008), and Salgado (2008), among others.

In the following sections geotechnical reliability-based design/analysis are applied to a footing foundation, an anchored sheet pile wall, a laterally loaded pile, and a Norwegian clay slope with spatial variability. Insights gained are highlighted, links with LRFD are discussed, and the complementary role that RBD can play towards LRFD is emphasized.

2. RBD OF FOUNDATION WIDTH AND LINKS WITH LRFD

The shallow strip footing in Figure 3 is subjected to a horizontal live load Q_h and centrally applied vertical live load Q_L and dead load Q_D. The base of the foundation is at a depth of 1.2 m in a silty sand with mean friction angle $\phi' = 26°$, cohesion $c' = 14$ kN/m^2, and unit weight $\gamma = 20$ kN/m^3. A negative correlation coefficient of –0.5 between c' and ϕ' is modelled as shown in the correlation matrix. The coefficients of variation (StDev/Mean) for c', ϕ', Q_h, Q_L and Q_D are 0.15, 0.10, 0.15, 0.15 and 0.10, respectively. The water table is far below the foundation. With respect to bearing capacity failure, the performance function (*PerFunc*) is:

$$PerFunc = q_u - q \qquad (6a)$$

where

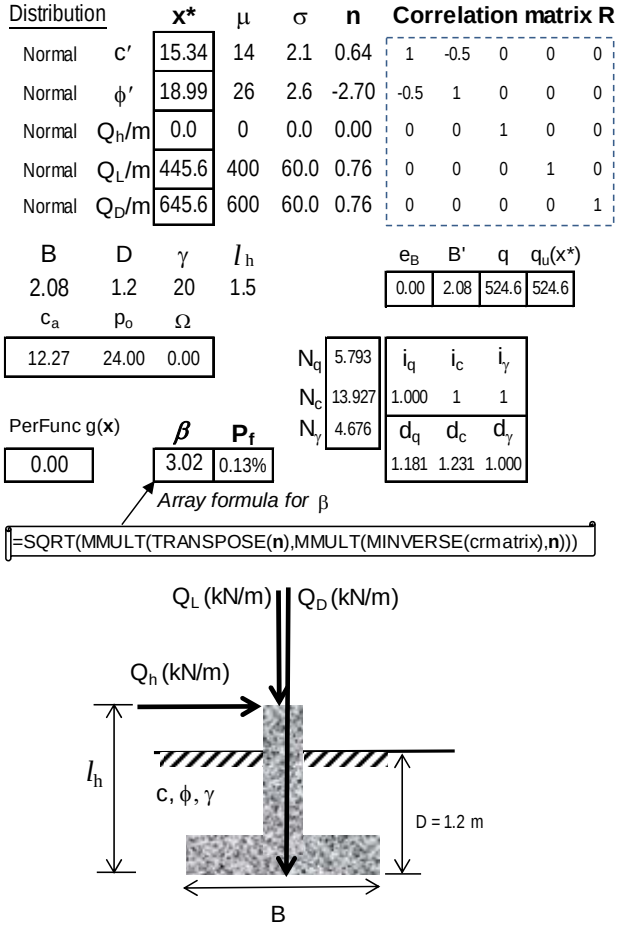

Figure 3: Reliability-based design obtains a foundation width B of 2.08 m for a target reliability index β of 3.0, using the Low and Tang (2007) Excel Solver FORM procedure. Other FORM software can also be used.

$$q_u = c'N_c d_c i_c + p_o N_q d_q i_q + \frac{B'}{2}\gamma N_\gamma d_\gamma i_\gamma$$

$$q = \left(Q_L + Q_D\right)/B' \qquad (6b,c)$$

in which q_u is the ultimate bearing capacity, q the applied bearing pressure, p_o the effective overburden pressure at foundation level, B′ the effective width of foundation, and N_c, N_q, and N_γ are bearing capacity factors, which are functions of the friction angle (ϕ') of soil. The six factors d_j and i_j in Eq. (6b) account for the depth effects of foundation and the inclination effect of the applied load. The formulas for N_c, N_q, and N_γ and the six depth and load inclination factor are based on Tables 4.5a and 4.5b of Bowles (1996).

2.1. Cases without horizontal load

For the case without horizontal load, Q_h is equal to 0.0 as shown in Figure 3. For a trial value of foundation width B, the Solver program of Microsoft Excel is invoked to minimize the β cell by automatically changing the five values under the column labelled **n**, subject to the constraint that the performance function cell labelled g(**x**) be equal to zero. After a few trial values of B, a B value of 2.08 m is found to achieve the target reliability index of β = 3.0. One may note the following with respect to the β value, the design point values **x***, and the sensitivity indicators **n** of Figure 3:

(i) The probability of failure P_f can be estimated from $P_f \approx \Phi(-\beta)$, where $\Phi(.)$ denotes the standard normal cumulative distribution. For β = 3.02 in Figure 3, $P_f \approx \Phi(-3.02)$ = 0.128%, which is in good agreement with 0.119%, 0.123% and 0.124% from three Monte Carlo simulations each with 800,000 trials using the @RISK software (http://www.palisade.com).

(ii) LRFD load factors and resistance factors can be back-calculated from a reliability-based design with respect to nominal resistance (which is lower than mean resistance) and nominal loads (which is higher than mean loads). The purpose of this study is not to calibrate factors for LRFD, but to investigate the links between RBD and LRFD and to suggest the complementary role that RBD can play towards LRFD. Hence methods of determining nominal resistance and nominal loads will not be discussed, and load and resistance factors will be back-calculated in this study with respect to the mean-value point. The insights gained in RBD and the ways RBD complements LRFD shown in this study are not affected by the different definitions of load and resistance factors in this study.

(iii) In Figure 3, the load factors (LF) with respect to mean values are x*/mean = 445.6/400 = 1.11 for live load Q_L, and 645.6/600 =1.08 for dead load Q_D. The design loads, Q_{Design}, is 445.5 + 645.5 = 1091, also equal to $q_u(x^*) \times B'$. The q_u value at mean-value point multiplied by B′ yields $Q_u(\boldsymbol{\mu})$ = 2038 kN/m. The ratio of Q_{Design} to $Q_u(\boldsymbol{\mu})$ is the resistance factor (RF) of 0.54 back-calculated from RBD.

(iv) Figure 3 is summarized as Case (a) in Figure 4. Case (b) in Figure 4 is for a higher target reliability index β of 3.5, resulting in a foundation width B of 2.3 m, which is bigger than Case (a)'s B = 2.08 m for a β of 3.0. The RF (0.48) is smaller and the LF (1.13, 1.09) slightly bigger for the higher target β and bigger required foundation width of Case (b) than those in Case (a).

(v) Cases (a) and (b) in Figure 4 are without horizontal loads. Based on the **n** values, The most pivotal parameter is ϕ′, followed by the vertical loads Q_L and Q_D. That the design values (x*) of c′ are higher than its mean value of 14 kPa is due to c′ being negatively correlated to ϕ′ and its less pivotal role than ϕ′.

When there is a horizontal load Q_h, as in Cases (c) and (d) of Figure 4, insights gained from

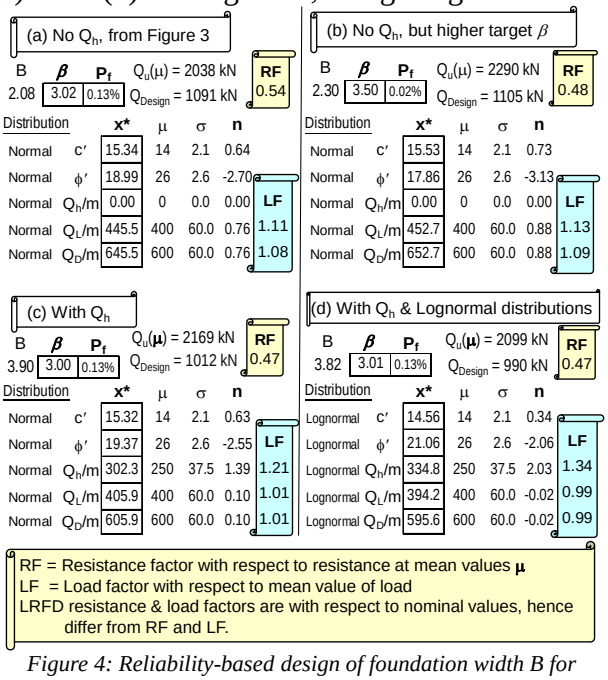

Figure 4: Reliability-based design of foundation width B for target reliability index β for four different scenarios.

reliability-based design suggest that direct application of load factors in LRFD could be misleading, as discussed next.

2.2. Cases with horizontal load Q_h

The load factors with respect to mean values of Q_L and Q_D are 1.01 for Case (c) and 0.99 for Case (d). This implies that the load factors of the vertical loads with respect to nominal loads (which are greater than mean loads) in LRFD will be less than 1.0. This apparent paradox of LF less than 1.0 is resolved if one notes that the vertical loads exert *both destabilizing and stabilizing effects* in the presence of horizontal load Q_h: increasing vertical loads will increase the vertical pressure q, but will also (when Q_h is present) enhance the bearing capacity q_u by offsetting the detrimental effects of horizontal load Q_h on the net foundation width B′ and the load inclination factors i_γ and i_q which appear in Eq. (6). The RBD Cases (c) and (d) show that the design point values **x*** (and implied load and resistance factors) are determined automatically in RBD and reflect parametric sensitivities, standard deviations, correlation structure, and probability distributions in a way that prescribed load and resistance factors in LRFD cannot.

3. RBD OF AN ANCHORED SHEET PILE WALL AND LINKS WITH LRFD

In the anchored sheet pile wall of Figure 5, the six random variables are assumed to be lognormally distributed. Given the uncertainties and correlation structure in Fig. 5, one wishes to find the required total wall height *H* so as to achieve a reliability index of 3.0 against rotational failure about the anchor point "*A*". The stability formulation was based on the free-earth support method.

The RBD shows that a total height H of 12.19 m would give a reliability index β of 3.0 against rotational failure. The **x*** values denote the *design point* on the limit state surface, and represent the most likely combination of parametric values that will cause failure. The expected embedment depth is $d = 12.19 - 6.4 - \mu_z = 3.39$ m. At the failure combination of

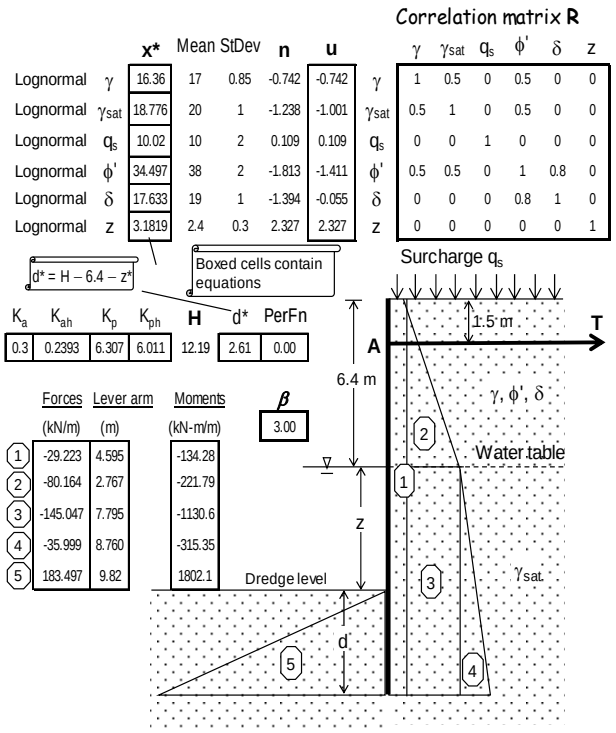

Figure 5: Reliability-based design of anchored wall: six correlated nonnormals, including the dredge level (and hence z and d).

parametric values the design value of *z* is $z^* = 3.182$, and $d^* = 12.19 - 6.4 - z^* = 2.61$ m. This corresponds to an 'overdig' allowance of 0.78 m. Unlike design codes (e.g. EC7), this 'overdig' is determined automatically, and reflects uncertainties and sensitivities from case to case in a way that specified 'overdig' cannot.

The **n** column indicates that, for the given mean values and uncertainties, rotational stability is, not surprisingly, most sensitive to ϕ' and the dredge level (which affects *z* and *d* and hence the passive resistance). It is interesting to note that at the design point where the six-dimensional dispersion ellipsoid touches the limit state surface, both unit weights γ and γ_{sat} (16.36 and 18.78 kN/m^3) are lower than their corresponding mean values, contrary to the expectation that higher unit weights will increase active pressure and hence greater instability. This apparent paradox is resolved if one notes that smaller γ_{sat} will (via smaller γ') reduce passive resistance, smaller ϕ' will cause greater active pressure and smaller passive pressure, and that γ, γ_{sat}, and ϕ' are logically positively correlated, and thus

modeled with positive correlation coefficients in the correlation matrix. It is also logical to assume a positive correlation between the soil angle of friction ϕ' and the interface friction angle δ between the soil and the sheet pile, and this also has been modeled in the correlation matrix.

In this case where some of the six parameters are (logically) correlated, as shown in Fig. 5, and where uncertainties in unit weights γ and γ_{sat} are modeled and single-source principle is to be observed, RBD can play a complementary role to LRFD and Eurocode 7 in automatically deciding whether the design values of γ and γ_{sat} should be lower or higher than their respective mean values.

Prior to RBD, the overturning and resisting moments evaluated at mean-value point are M_R = 4324 kNm/m, and M_o = 1629 kNm/m. After RBD design, the diminished resisting moment is equal to the amplified overturning moment, both equal to 1802 kNm/m. This means that the resistance factor (with respect to moments at mean-value point) is 1802/4324 = 0.42, and the load factor (in this case overturning moment factor) is 1802/1629 = 1.11. (The corresponding LRFD resistance factor is higher than 0.42, and the LRFD load factor is smaller than 1.11, because the RF and LF in LRFD are defined in terms of nominal resistance (< 4324 kNm/m) and nominal loads (>1629 kNm/m)). Note that in this example the overturning and resisting moments are affected probabilistically in a complexly intertwined manner due to uncertainty in dredge level z, parametric correlations, and single-source principle on the unit weights. The back-calculated RF and LF will differ from the above values of 0.42 and 1.11 if the uncertainty model (number and type of random variables, parametric correlations, probability distributions) is different. RBD can play a complementary role to LRFD by directly basing the design on the uncertainty model for a target reliability index or probability of failure, and, if desired, providing back-calculated RF and LF.

If desired, the original correlation matrix can be modified in line with the equivalent normal transformation, as suggested in Der Kiureghian and Liu (1986). For the cases illustrated herein, the correlation matrix thus modified differs only very slightly from the original correlation matrix. Hence, for simplicity, the examples of this study retain the original unmodified correlation matrices.

3.1 Positive reliability index only if the mean-value point is in the safe domain

In Fig. 5, if a trial *H* value of 10 m is used, and the entire **n** column given their initial values of 0.0, the **x*** column will display the respective mean value, and the performance function *PerFn* exhibits a negative value of –437.28, meaning that, for the input *H* of 10 m, the equivalent mean value point is already inside the unsafe domain. Upon Solver optimization with constraint *PerFn* = 0, a β index of 1.36 is obtained, which should be regarded as a negative index, i.e., –1.36, meaning that the *unsafe* mean value point is at some distance from the nearest safe point on the limit state surface that separates the safe and unsafe domains. In other words, the computed β index can be regarded as positive only if the performance function (*PerFn*) value is positive at the mean value point. For the case in hand, the mean value point (prior to Solver optimization) yields a positive *PerFn* for H > 10.6 m. The computed β index increases from about 0 (equivalent to a factor of safety equal to 1.0) when H is 10.6 m to 3.0 when H is 12.19 m for the statistical inputs of Fig. 5.

4. RBD OF A LATERALLY LOADED PILE WITH SPATIAL VARIABILITY OF C_U

The steel tubular pile in Fig. 6 is embedded 23 m in the stiff overconsolidated clay with average undrained shear strength c_u = 150 kN/m^2 near sea bed, and protrudes 26 m above the sea bed. The Matlock p-y curves for clays are nonlinear, exhibit strain-softening, and vary with depth. The calculated pile deflection (y_i) at seabed level (where z = 0) is 0.06 m. The pile head deflection (at 26 m above the seabed) at mean value of P_H (421 kN) is 0.994 m, or about 1 m.

Reliability analysis with spatial variation of the c_u values was described in Low and Phoon (2015), including RBD for both moment capacity and deflection limit states. For the bending moment limit state, at the most probable failure point (where the hyperellipsoid touches the limit state surface) the value of the lateral load at pile head is P_H = 580.3 kN, i.e., at $1.513\sigma_{PH}$ from the mean value of P_H, while the 31 autocorrelated c_u values deviates only very slightly from their mean values. This is not surprising given the e = 26 m cantilever length above the seabed; in fact the maximum bending moment occurs at a depth of only 1.36 m below the seabed, or 27.36 m from the pile head. Hence, for the case in hand, pile yielding caused by bending moment is more sensitive to the applied load at pile head than to the uncertainty of the shear strength below seabed. However, separate reliability analysis for cases where the lateral load acts on pile head near ground surface (with zero cantilever length) indicates that the response is sensitive to both the lateral load at pile head and the soil shearing resistance within the first few meters of the ground surface. The different sensitivities from case to case is automatically reflected in reliability analysis aiming at a target index value, but will be difficult to consider in codes based on LRFD or EC7. The useful insights offered by RBD to complement LRFD and EC7 design are obvious, because RBD automatically reflects such different c_u sensitivities from case to case with different protruding pile lengths above seabed.

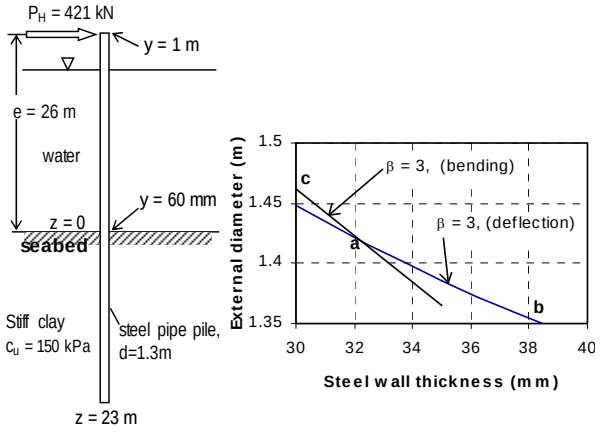

Figure 6: RBD of a laterally loaded pile for bending and deflection limit states with a relability index β of 3.0

5. SLOPE RELIABILITY ANALYSIS WITH SPATIAL VARIABILITY

A clay slope in Norway (Fig. 7) was analyzed in Low et al. (2007) using Spencer method and FORM, and with modeling of 24 spatially autocorrelated soil unit weight values and 24 spatially autocorrelated anisotropic undrained shear strength values.

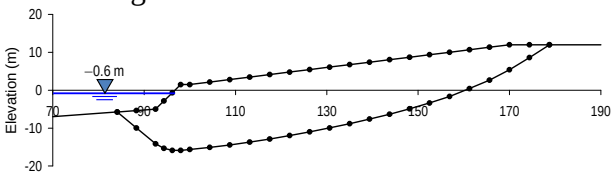

Figure 7: Slope reliability analysis with spatial variability (Low, Lacasse and Nadim 2007)

The design point obtained by Excel Solver represents the most probable combination of the 24 values of c_u and the 24 values of γ which would cause failure. As expected for resistance parameters, the 24 values of undrained shear strength c_u at the design point are all lower than their respective mean values. Most design-point values of unit weight γ^* are also above their mean value μ_γ, as expected for loading parameters, but, interestingly, there are some design-point values of γ near the toe which are below their mean values. The implication is that the slope is less safe when the unit weights near the toes are lower. This implication can be verified by deterministic runs using higher γ values near the toe, with resulting higher factors of safety. It would be difficult for design code committee to recommend load factors such that the design values of γ are above the mean along some portions of the slip surface and below their mean along other portions. In contrast, the design point is located automatically in FORM analysis using the Excel Solver constrained optimization program, and reflects sensitivity and the underlying statistical assumptions from case to case in a way that code-specified load factors cannot.

6. GEOTECHNICAL SORM, SYSTEM FORM, AND RESPONSE SURFACE

Other geotechnical studies of FORM, system FORM, SORM, and response surface methods (as a link between stand-alone numerical packages and the spreadsheet-based FORM and SORM procedures) are presented in Low and Duncan (2013), Low and Einstein (2013), Low (2014), and Low (2015).

7. CONCLUSIONS

The geotechnical examples of reliability-based design in this study show that RBD can play a complementary role to LRFD when (i) A target reliability index or probability of failure is aimed at; (ii) The effects of loads or unit weights are both destabilizing and stabilizing, as illustrated in Sections 2, 3 and 5; (iii) Geological spatial variability and parametric correlations are modelled such that back-calculated load and resistance factors are not unique but depend on the details of modeling (e.g. the laterally loaded pile of Section 4).

8. REFERENCES

Ang, H.S., and Tang, W.H. (1984). Probability Concepts in Engineering Planning and Design, vol. 2, Decision, Risk, and Reliability. John Wiley, New York.

Bathurst, Richard J.; Allen, Tony M.; Nowak, Andrzej S. (2008). “Calibration concepts for load and resistance factor design (LRFD) of reinforced soil walls”, *Can. Geotech. J.*, 45(10): 1377-1392.

Der Kiureghian, A. & Liu, P.L. (1986). “Structural reliability under incomplete probability information.” J. Engrg, Mech., ASCE, 112(1), 85-104.

Fenton, Gordon A., Griffiths D.V., and Zhang, Xianyue (2008). “Load and resistance factor design of shallow foundations against bearing failure.” *Can. Geotech. J.* 45: 1556–1571.

Foye, K.C., Salgado, R. and Scott, B. (2006). “Resistance Factors for Use in Shallow Foundation LRFD”, *Journal of Geotech. and Geoenviron. Engrg*, 132(9), 1208–1218.

Haldar, A., and Mahadevan, S. (1999). *Probability, Reliability and Statistical Methods in Engineering Design*. John Wiley, New York.

Hasofer, A.M., and Lind, N.C. (1974). “Exact and invariant second-moment code format”, *Journal of Engineering Mechanics*, 100: 111–121, ASCE, New York.

Low, B.K., and Tang, Wilson H. (2004). “Reliability analysis using object-oriented constrained optimization.” *Structural Safety*, Elsevier Science Ltd., Amsterdam, 26(1), 69-89.

Low, B.K., and Tang, Wilson H. (2007). “Efficient spreadsheet algorithm for first-order reliability method.” *Journal of Engineering Mechanics*, ASCE, 133(12), 1378-1387.

Low, B.K., Lacasse, S. & Nadim, F. (2007). “Slope reliability analysis accounting for spatial variation”, *Georisk: Assessment and Management of Risk for Engineered Systems and Geohazards*, Taylor & Francis, London, Vol. 1, No. 4, pp.177-189.

Low, B.K. & Duncan, J.M. (2013). "Testing bias and parametric uncertainty in analyses of a slope failure in San Francisco Bay mud". *Proceedings of Geo-Congress 2013*, ASCE, March 3-6, San Diego, 937-951.

Low, B.K. & Einstein, H.H. (2013). “Reliability analysis of roof wedges and rockbolt forces in tunnels”. *Tunnelling and Underground Space Technology*, Elsevier, 38, 1–10.

Low, B.K. (2014). “FORM, SORM, and spatial modeling in geotechnical engineering”, *Structural Safety*, Elsevier, 49: 56–64.

Low, B.K. (2015), “Reliability-based design: practical procedures, geotechnical examples, and insights”, Chapter 9 of Risk and Reliability in Geotechnical Engineering, Edited by Kok-Kwang Phoon, Jianye Ching, CRC Press, 624 pages.

Low, B.K. and Phoon, K.K. (2015). “Reliability-based design and its complementary role to Eurocode 7 design approach”, *Computers and Geotechnics*. (In Press)

Melchers, R.E. (1999). Structural Reliability Analysis and Prediction, 2nd ed., John Wiley, New York.

Rackwitz, R., and Fiessler, B. (1978). “Structural reliability under combined random load sequences”, Computer Structures, 9(5): 484–494.

Salgado, R. (2008). *The engineering of foundations*, McGraw Hill, Boston.

Shinozuka, M. (1983). “Basic analysis of structural safety”, *Journal of Structural Engineering*, ASCE, 109(3): 721–740.